Determination of Flow Curves by Stack Compression Tests and Inverse Analysis for the Simulation of Hot Forming

B. Hochholdinger[1], H. Grass[2], A. Lipp[2], P. Hora[1]
[1] Institute of Virtual Manufacturing, ETH Zurich, Zurich, Switzerland
[2] BMW AG, Munich, Germany

Summary: Due to the increasing number of body-in-white parts that are manufactured by hot forming of boron alloyed sheet metal (22MnB5), the demand for a virtual representation of this specific manufacturing process is evident. For a realistic simulation of hot stamping processes, the accurate modeling of the flow stress as function of strain, strain rate and temperature is essential.
In the last years a large varity of empirical-analytical as well as physically based models for the yield stress has been proposed. Three existing models that have shown a good capability to represent the flow behavior of 22MnB5 in recent publications are presented and fitted to the experimental data. The underlying experimental data for the determination of the flow stress is obtained by stack compression tests, which were conducted in a high-speed deformation dilatometer.
In a first step the model parameters are fitted to the experimental flow curves without considering the friction, which inherently is present in a compression test. Since the friction between die and specimen has significant influence on the state of stress within the specimen, an inverse, simulation-based approach for the determination of the model parameters is employed. For this purpose a simple 2D FE model for each test configuration is set up. The resulting "friction-free" yield stress is up to 15% lower than the one without considering friction. Regarding the models considered, the approach developed by TONG and WAHLEN, which is based on the ZENER-HOLLOMON parameter and a HOCKETT-SHERBY type formulation, provides the best fit of the experimental data.

Keywords:

flow stress, 22MnB5, hot forming, stack compression test, parameter identification, inverse modeling

© 2009 Copyright by DYNAmore GmbH

1 Introduction

Press hardening of sheet metal for the production of ultra high strength structural steel parts is a well established process in the automotive industry today. The permanent demand for weight reduction and improved crash performance of the body-in-white will most likely lead to an even higher fraction of crash relevant structural parts that are manufactured by the press hardening process. Due to the fact that press hardening is an expensive process regarding cycle times, energy consumption, cooling of the tools, etc. compared to classical cold forming, it is essential that the process and tool layout are done virtually prior to money and time consuming real tryout loops. In contrast to cold sheet metal forming press hardening can not be considered isothermal, which means that the temperature field must not be neglected in the simulation and therefore a thermomechanically coupled solution strategy has to be followed.
For the coupled IBVP (Initial Boundary Value Problem) the simulation engineer has to define not only mechanical and thermal initial and boundary conditions but also the temperature dependency of the mechanical parameters, as e.g. for friction and yield stress. Especially for the direct press hardening process, where the blank is formed and quenched simultaneously within one process step, the definition of the flow stress as a function of strain but also of strain rate and temperature is essential in order to achieve reliable results.
In the subsequent chapters the experimental procedure for the determination of the strain, strain rate and temperature dependency of the yield stress is presented. Furthermore different mathematical models are fitted to the experimental results and the capability of the models to reproduce the test data is compared. In order to account for the influence of friction on the test results, an inverse, simulation-based method to identify the model parameters is presented.

2 Material properties and experimental setup

The material examined is phs-ultraform®, which is the trade name for steel grade 22MnB5 from voestalpine AG. The experiments for the determination of the plastic flow properties were conducted in a high-speed deformation dilatometer “Bähr DIL805A/D” by upsetting tests.
Currently 22MnB5 is more or less the only steel grade used for parts that are manufactured by press hardening in the automotive industry. 22MnB5 is a low carbon steel that contains a small amount of boron in order to enhance the quenching behavior in such way that even for moderate cooling rates (greater than 30 K/s) a fully martensitic microstructure is obtained. The chemical composition of phs-ultraform® as stated by FADERL [1] is listed in table 1. The distinguishing feature of phs-ultraform®

Table 1: Chemical composition of phs-ultraform® from [1]

C	Si	Mn	Cr	B
0.22 %	0.2 %	1.2 %	0.25 %	30 ppm

compared to 22MnB5 steel from other steel suppliers is mainly its zinc coating, which provides cathodic corrosion protection for the base material. For details on the zinc coating, its corrosion resistance and the chemical processes of and in the coating during quenching see FADERL[1] and LAUMANN [2].
The tested material is sheet metal with a thickness of 1.83 mm. In order to get a sufficient initial height of the cylindrical specimen of min. 5.0 mm, 3 circular slices with a diameter of 5.0 mm are stacked upon each other. The slices were cut out of a sheet by wire-electro discharge machining and glued together. When stacking and glueing the sheet slices, care has to be taken to get reproducable, cylindrical specimens. In order to minimize the heat flow into the ceramic dies (Al_2O_3) and hence to ensure a homogeneous temperature distribution within the specimen, molybdenum platelets with a diameter of 8 mm and a thickness of 0.1 mm were attached to the upper and lower face of the test sample. As lubricant between the molybdenum platelets and the specimen MOLYKOTE® HSC Plus paste was used. The temperature was measured with a Ni/NiCr thermocouple, which was spot-welded to the specimen. Figure 1 shows the setup of a specimen, which is ready to be tested. Regarding the experimental procedure it is important that the material undergoes a temperature history as close as possible to the real process. Therefore a temperature-time program according to figure 2 was used in the experiments. After

© 2009 Copyright by DYNAmore GmbH

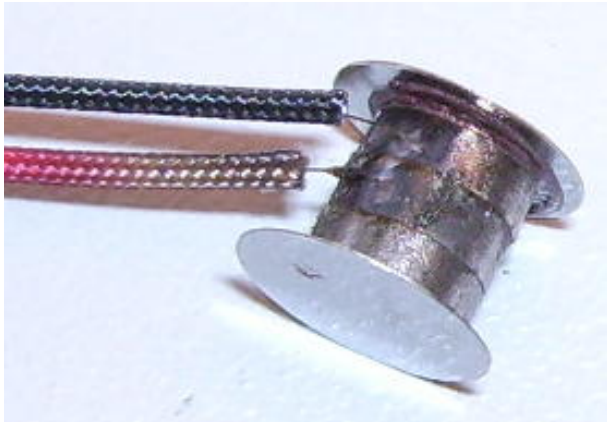

Figure 1: Upsetting specimen “ready-to-test”: 3 stacked sheet slices, lubricant, molybdeneum platelets and Ni/NiCr thermocouple.

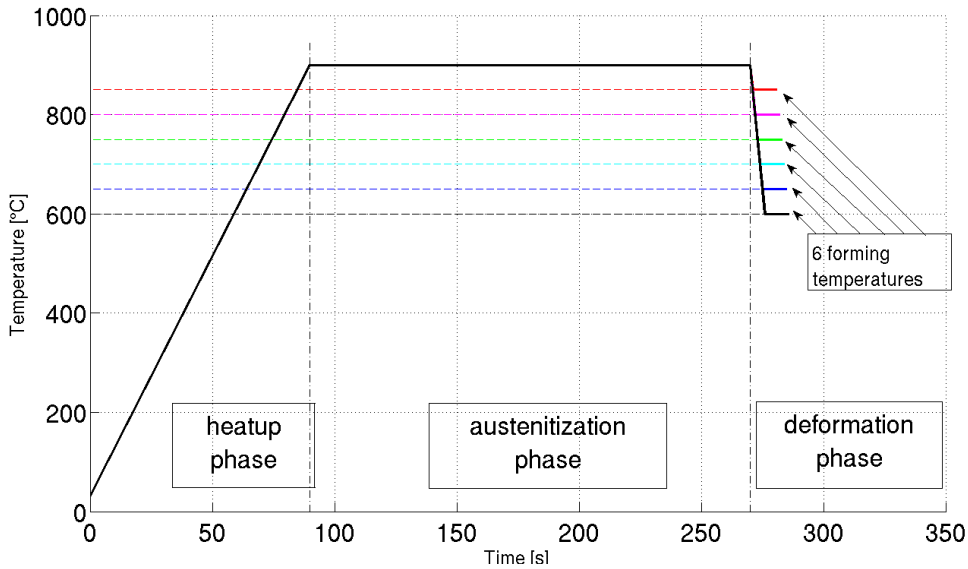

Figure 2: Temperature versus time program used for the experiments.

applying a vacuum to the test chamber of approx. 10^{-4} mbar, the specimen is heated up by inductive heating to a temperature of 900 $°C$ within 90 s. Then the temperature is held constant for another 180 s to achieve a fully austenized microstructure. Afterwards the specimen is cooled down to the actual test temperature with a cooling rate of 50 K/s. In order to ensure a constant cooling rate of 50 K/s, helium gas is applied onto the sample. Before finally applying the deformation, the test temperature is held constant for one second to allow the control unit of the dilatometer to adjust the preset temperature exactly. Then the deformation is applied with a constant strain rate at a constant temperature up to a true strain of 0.5. Since the plastic work during the deformation is almost completely converted into heat, the temperature

Table 2: Number of vaild test results for different configurations of strain rate and forming temperature.

$T/\dot{\varepsilon}$	0.1 1/s	1.0 1/s	5.0 1/s
600 $°C$	3	4	3
650 $°C$	5	3	3
700 $°C$	6	4	3
750 $°C$	6	4	3
800 $°C$	5	8	3
850 $°C$	4	3	3

© 2009 Copyright by DYNAmore GmbH

in the specimen is not constant. If the measured temperature deviates more than $\pm 4\ ^{\circ}C$ from the designated temperature the results of the experiment are not taken into account for further evaluations. Table 2 shows the complete test matrix and the number of valid experiments for the 18 configurations. Since the temperature control of the dilatometer is quite sensitive, much more than 3 experiments had to be done to get at least 3 valid results per configuration.

3 Experimental Results

Figure 3 shows exemplarily the experimental results for strain rate $1.0\ 1/s$ for test temperatures $T = 650,\ 750$ and $850\,^{\circ}C$, respectively. For each test configuration the individual curves of the "valid" experiments (thin line) as well as the averaged curve (thick line) are displayed. Accordingly, in figure 4 the experimental results for the strain rates $\dot{\varepsilon} = 0.1,\ 1.0$ and $5.0\ 1/s$ at a test temperature of $T = 650\,^{\circ}C$ are displayed. The oscillations within the individual stress curves are mainly due to fluctuations of the temperature during the compression of the specimen.

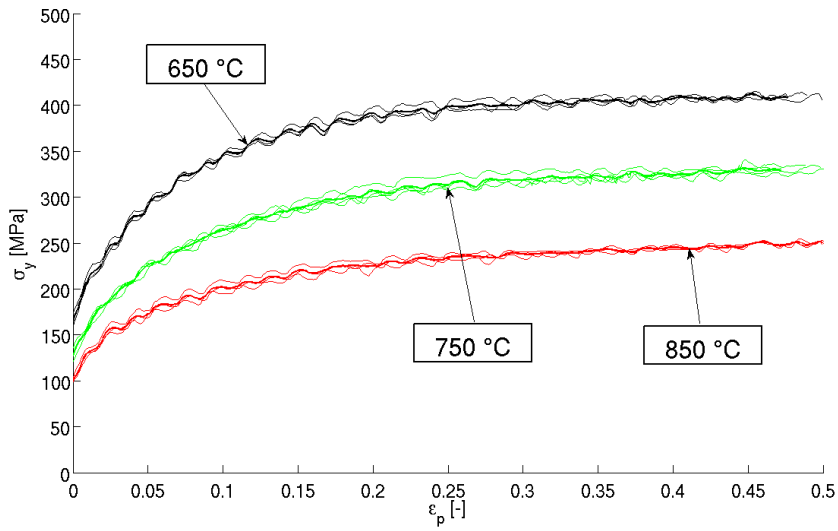

Figure 3: Flow stress curves for 3 test temperatures at a constant strain rate $\dot{\varepsilon} = 1.0\ 1/s$.

4 Mathematical Modeling

During the last years several papers have been published presenting different models for the flow stress of 22MnB5 as a function of strain, strain rate and temperature. The experimental results were either obtained by hot tension tests as for example in BROSIUS [3] and MERKLEIN [4] or by compression tests using conventional (ERIKSSON [5], NADERI [6]) or stacked specimens (BURKHARDT [7]).
According to BARIANI [8] one can generally distinguish between empirical anlytical, physically-based and empirical non-analytical models. Empirical analytical models deploy phenomenological derived expressions to model the flow stress as a function of macroscopic process parameters. The material constants within such formulations do not have a physical meaning and are usually determined by regression analysis. In contrast to empirical analytical models, the so-called physically-based models are functions of internal variables, which reflect the initial physical (micro-)structure of the material as well as its evolution. Empirical non-analytical models, which usually use a neural network-based approach instead of an explicit analytical expression for the flow stress, are not considered in this paper. For practical applications empirical analytical models – due to their simplicity – are often favored over physically-based models. The latter require complex and expensive experiments to determine the internal variables with an adequate accuracy. It is also popular to use a combination of both approaches. When the parameters are fitted to the experimental data for such models, the resulting values for the parameters with a

© 2009 Copyright by DYNAmore GmbH

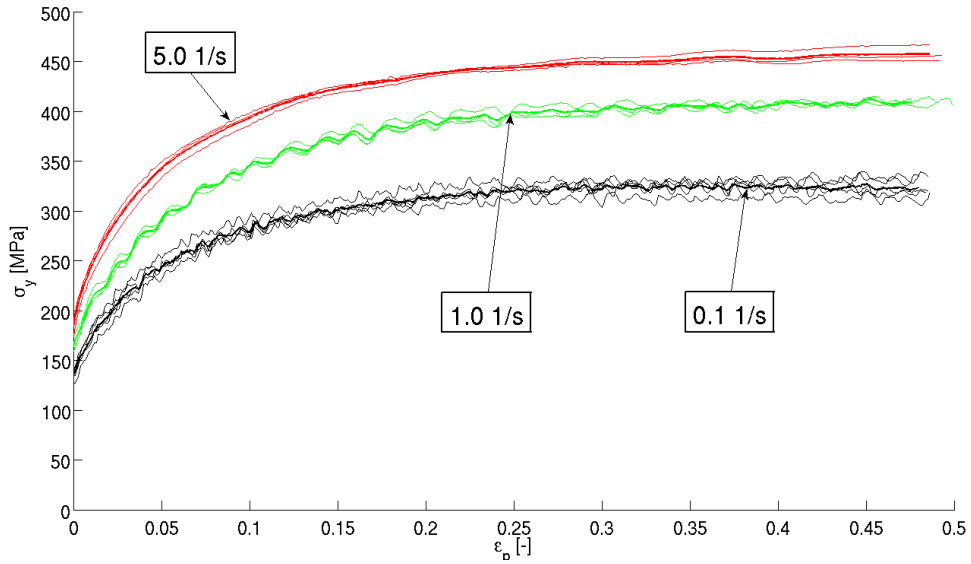

Figure 4: Flow stress curves for 3 strain rates at a constant test temperature $T = 650\,°C$.

physical meaning can be checked versus values from literature. This provides a first check regarding the validity of the model and/or the fitting procedure, respectively. In this paper three models, which have shown a good capability to reproduce the experimental data for 22MnB5, have been selected and evaluated.

4.1 Norton-Hoff Model

The first model considered is a modified Norton-Hoff approach as described in BROSIUS [3]. As in most models that follow the empirical-analytical approach, the components that account for the strain, strain rate and temperature dependency of the flow stress are multiplied with each other. The original NORTON-HOFF model has the following form.

$$\sigma_y(\varepsilon_p, \dot{\varepsilon}_p, T) = K_\varepsilon \cdot K_{\dot{\varepsilon}} \cdot K_T = K\varepsilon_p^n \cdot \dot{\varepsilon}_p^m \cdot e^{\frac{\beta}{T}} \tag{1}$$

In order to correctly reproduce the initial yield stress and to account for the temperature dependency of K_ε and $K_{\dot{\varepsilon}}$ equation 1 has been extended by defining parameters n and m as a function of temperature T, respectively (see equation 2 as defined in [3]).

$$\sigma_y(\varepsilon_p, \dot{\varepsilon}_p, T) = K\,(b+\varepsilon_p)^{n_0 \cdot e^{-c_n(T_i - T_0)}} \cdot \dot{\varepsilon}_p^{m_0 \cdot e^{c_m(T_i - T_0)}} \cdot e^{\frac{\beta}{T}} \tag{2}$$

Consequently 7 parameters (K, b, n_0, c_n, m_0, c_m, β) have to be determined in order to approximate the flow stress with this model.

4.2 Nemat-Nasser Model

The second model, which is applied to fit the experimental data, is a physically-based model and was developed by NEMAT-NASSER [9]. This model can be used to approximate the flow behavior of both fcc as well as bcc polycrystals and was initially employed to pure tantalum and oxygen free, high conductivity (OFHC) copper. As shown by ÅKERSTRÖM [10] the model is also capable to reproduce the flow stress of 22MnB5 in its austenitic (fcc) state. The expression of the flow stress as a function of the strain, strain rate and the temperature uses various material constants on the dislocation scale and has the following form.

$$\sigma_y = \sigma_0 \left\{ 1 - \left[-\frac{kT}{G_0} \left(\ln \frac{\dot{\varepsilon}}{\dot{\varepsilon}_0} + \ln f(\varepsilon_p, T) \right) \right]^{1/q} \right\}^{1/p} \cdot f(\varepsilon_p, T) + \sigma_a^0 \cdot g(\varepsilon_p, d_g, \ldots) \tag{3}$$

© 2009 Copyright by DYNAmore GmbH

Where σ_0 is an effective stress, which has to be determined empirically, k is the BOLTZMAN constant ($k = 1.3806505 \cdot 10^{-23} J/K$), parameters p and q define the shape of the energy barrier, G_0 is the magnitude of the activation energy and $\dot{\varepsilon}_0$ is a reference strain rate related to the density and the average velocity of the mobile dislocations and the barrier spacing (see [9] for details). Depending on the lattice structure – fcc or bcc – the function $f(\varepsilon_p, T)$ takes a different expression. In ÅKERSTRÖM [10] the formulation according to equation 4, which was initially used for OFHC copper, is also used for 22MnB5 in its austenitic state.

$$f(\varepsilon_p, T) \approx 1 + a_0 \left[1 - \left(\frac{T}{T_m} \right)^2 \right] {\varepsilon_p}^{1/2} \tag{4}$$

The last term $\sigma_a^0 \cdot g(\varepsilon_p, d_g, ...)$ defines the athermal part of the flow stress and may be approximated by

$$\sigma_a^0 \cdot g(\varepsilon_p, d_g, ...) \approx \sigma_a^0 \cdot {\varepsilon_p}^n \tag{5}$$

For a thorough treatment of all parameters in equations 3 - 5 please refer to NEMAT-NASSER [9].
Even though this model is physically-based the 8 model parameters σ_0, (k/G_0), $\dot{\varepsilon}_0$, a_0, q, p, σ_a^0 and n are determined by regression analysis.

4.3 Tong-Wahlen Model

The last model considered contains both, physically-based as well as empirical parameters. It is based on the so-called ZENER-HOLLOMON parameter Z, which defines a temperature compensated strain rate. In WAHLEN [11] the following relation for connecting strain rate, temperature and stress is proposed.

$$Z = \dot{\varepsilon}_p \, e^{\frac{Q}{RT}} = K \sigma^n \tag{6}$$

With Q being the activation energy and $R = 8.314472 J/molK$ the universal gas constant. Solving equation 6 for the stress leads to

$$\sigma_y = K^{-1/n} \left[\dot{\varepsilon} \, e^{\frac{Q}{RT}} \right]^{1/n} = A \left[\dot{\varepsilon} \, e^{\frac{Q}{RT}} \right]^m . \tag{7}$$

In order to include the strain dependency of the flow stress as well as softening effects because of either recovery or recrystallization TONG [12] proposed the following extension of equation 7.

$$\sigma_y(\varepsilon_p, \dot{\varepsilon}_p, T) = A \left[\dot{\varepsilon}_p \, e^{\frac{Q}{RT}} \right]^m \cdot \left[1 + \alpha \, e^{-c\left(\varepsilon_p - \varepsilon_0\right)^2} \right] \cdot \left[1 - \beta \, e^{-N \varepsilon_p^n} \right] \tag{8}$$

Where the second term accounts for softening effects and the third term, which is a HOCKETT-SHERBY type formulation, accounts for the strain hardening. Since the experimental results did not show significant reductions of the flow stress the model was simplified in such way that the second term is neglected. Furthermore, in order to account for an increasing strain rate sensitivity with increasing temperature, BURKHARDT[7] defines the strain rate exponent m as a linear function of the temperature T. This leads to the following form of the TONG-WAHLEN model.

$$\sigma_y = A \left[{\dot{\varepsilon}_p}^{m_1 (T - T_0)} \cdot e^{\frac{m_2 Q}{RT}} \right] \cdot \left[1 - \beta \, e^{-N \varepsilon_p^n} \right] \tag{9}$$

For 22MnB5 the activation energy Q is assumed to be equal to $280 kJ/mol$. Consequently, equation 9 contains 7 model parameters (A, m_1, m_2, T_0 , β, N, n) that have to be determined by regression analysis.

© 2009 Copyright by DYNAmore GmbH

5 Regression Analysis

For the direct identification of the model parameters, two different optimization algorithms within MATLAB® are used. The first function applied is `fminsearch`, which uses the NELDER-MEAD simplex algorithm – a direct search method that does not use numerical or analytic gradients. The objective for the optimization procedure is to minimize the residual between experimental data and model result. The residual is defined as the proportionally weighted mean square error (MSE), which for this problem is defined by the following expression.

$$MSE = \sum_{k=1}^{18} \left[\frac{1}{p} \sum_{i=1}^{p} \left(\frac{\sigma_i^{exp} - \sigma_i^{mod}}{\sigma_i^{exp}} \right)^2 \right] \tag{10}$$

where N is the number of different strain rate/temperature configurations considered and p is the number of points in each configuration, respectively. The second function employed is `nlinfit`, which directly minimizes the mean square error of the model prediction compared to the test data using the LEVENBERG-MARQUARDT (LM) algorithm. In general the gradient-based LM algorithm needs much less iterations to find a converged solution than the simplex algorithm. On the other hand the convergence behaviour of `fminsearch` is more robust regarding variations of the starting values for the unknown material parameters. If the same starting vector is used, both algorithms converge – from an engineering point of view – to the same set of model parameters.
Comparing the convergence behavior for the 3 models considered, it is obvious, but nevertheless should be mentioned, that the less parameters have to be determined the easier a converged solution is obtained. In table 3 the mean error (ME) in $[MPa]$ and $[\%]$, the root mean square error (RMSE) as well as the coefficient of determination (R^2) of the nonlinear regression analysis for all models are tabulated.
With the model by TONG-WAHLEN (eq. 9) the best fit of the experimental data can be realized. As

Table 3: Results of the nonlinear regression analysis for the different models.

Model	ME $[MPa]$	ME $[\%]$	RMSE $[MPa]$	R^2 $[-]$
Norton-Hoff	11.1	3.9	13.8	0.977
Nemat-Nasser	13.1	4.7	16.8	0.966
Tong-Wahlen	8.4	3.0	10.5	0.987

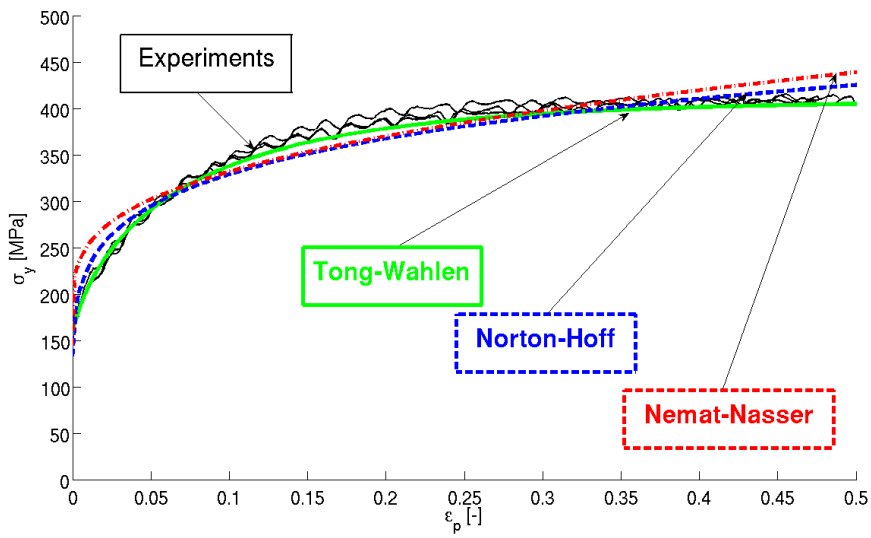

Figure 5: Flow stress curves of the 3 models and the experiments for $T = 650\,°C$ and $\dot{\varepsilon} = 1.0\ 1/s$.

© 2009 Copyright by DYNAmore GmbH

can be seen in figure 5 the NORTON-HOFF and the NEMAT-NASSER model are not able to describe the saturation of the flow stress at higher values of the effective plastic strain very well. Mainly due to the HOCKETT-SHERBY term in equation 9 the TONG-WAHLEN model has a good capability to match the experimental stress values also for higher strains.

6 Parameter Identification by an Inverse Method

One major problem of the fitting procedure described in chapter 5 is the neglection of the influence of friction, which is present in the compression tests. Even though a high temperature resistant lubricant is used, the specimens show the typical bulging behavior (fig. 6), which indicates that the influence of friction could not be eliminated. That means that the stress state in the specimen is not a uniaxial one

Figure 6: Undeformed and deformed specimen.

and hence the resulting flow curves, which are obtained by assuming a uniaxial state of stress, are too high. In order to overcome this problem an inverse approach is chosen, using one-to-one simulations of the different compression tests.

6.1 Simulation of Compression Tests

For the simulation of the compression tests, a simple 2D LS-DYNA® [13] model using axisymmetric elements is set up. Figure 7 shows the quarter-model consisting of 30 quadrilateral elements in the deformed state, when friction between die and specimen is considered in the simulation. In a first step

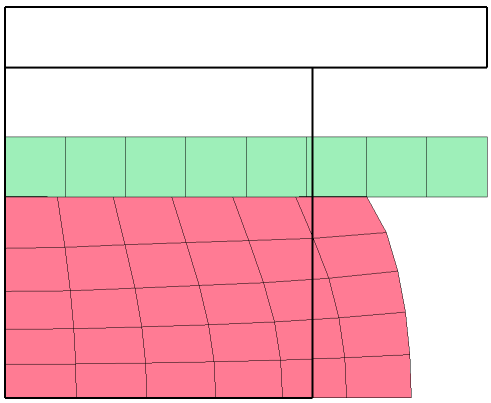

Figure 7: Quarter FE model of compression test in the deformed (mesh) and undeformed state (edge).

© 2009 Copyright by DYNAmore GmbH

– in order to ensure that the simple FE model is able to reproduce the experiment with adequate accuracy – simulations were set up without friction, using directly the experimental flow curves as input for the material model. The resulting force-displacement curves were compared with the ones measured in the experiments. From these first simulations it got obvious that it is necessary to include the small variations of the initial specimen height in the FE model in order to match the experimental results with a high accuracy.
Since it was unfortunately not possible to measure the diameter of the specimen online during the experiment, the final, deformed geometry was compared with simulation results using various coefficients of friction. From that a Coulomb friction coefficent $\mu = 0.2$ was determined, which was used for all subsequent simulations.

6.2 Optimization Procedure

Since the TONG-WAHLEN model showed the highest capabilty to fit the experimental data, this model was chosen for the simulation-based fitting procedure. For each of the 18 configurations listed in table 2 a specific, isothermal FE model was set up. The optimization was defined within LS-OPT® [14], which uses a successive response surface method (SRSM) in order to minimize the MSE (eq. 10) of the force-displacement curves from the simulations and the experiments. In LS-OPT® linear polynomial response surfaces and a D-optimal approach for the point selection were selected. Hence 13 simulation runs per configuration were necessary to determine the 7 model parameters. After 14 iterations ($14 \cdot 18 \cdot 13 = 3276$ runs), a converged solution was obtained. The sheer amount of simulations necessary underlines the fact that an approach which follows the maxime “A simple model is a better model” is still adequate. Alternatively an approach as proposed by ÅKERSTRÖM [10] using simultaneous cooling and compression experiments for the parameter identification is probably more effective regarding the number of simulation runs necessary. Figure 8 shows the difference for the TONG-WAHLEN model if

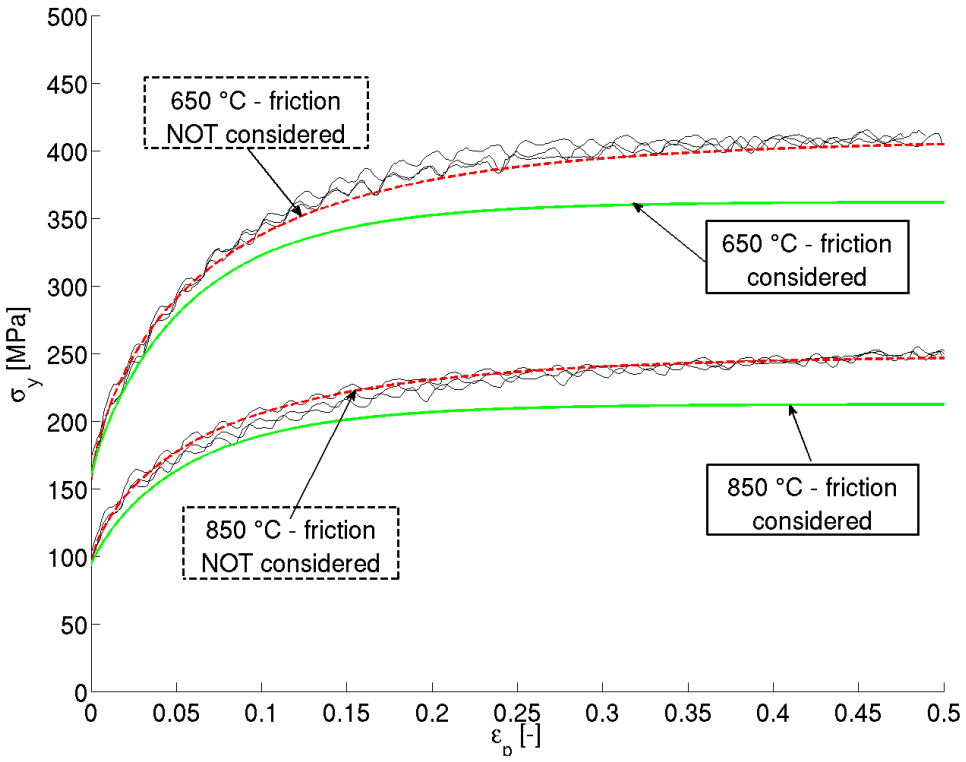

Figure 8: Flow curves of experiments and TONG-WAHLEN model with and without consideration of friction for $\dot{\varepsilon} = 1.0\ 1/s$.

fitted with and without considering the influence of friction. The resulting “friction-free” yield stress is up to 15% lower than the one without considering friction.

© 2009 Copyright by DYNAmore GmbH

7 Conclusions

For the determination of the flow stress as function of strain, strain rate and temperature, stack compression tests have been performed. Three different mathematical models are employed to fit the experimental data. From the models considered, an approach developed by TONG and WAHLEN, which is based on the ZENER-HOLLOMON parameter and a HOCKETT-SHERBY type formulation, provided the best fit of the experimental data. Furthermore, in order to exclude the influence of friction, which is inherently present during compression tests, on the flow curves an inverse parameter identification is performed. For this purpose a simple 2D FE model for each test configuration is set up. The inclusion of friction in the fitting procedure results in a significant reduction of the effective yield stress and must therefore not be negelected for the determination of the model parameters.

8 Acknowledgement

The kind support of this work by the BMW Group ist gratefully acknowledged. Also many thanks to Dr. R. Grüebler from the Institute of Virtual Manufacturing (ETH Zurich) for the technical support regarding the experiments.

9 Literature

[1] J. Faderl and K. M. Radlmayr. ultraform und ultraform_phs innovation made by voestalpine. In *1. Erlanger Workshop Warmblechumformung*, pages 130–149, 2006.

[2] T. Laumann and M. Pfestdorf. Potential verzinkter Warmumformteile für den Einsatz in der Rohkarosserie. In *2. Erlanger Workshop Warmblechumformung*, pages 149–162, 2007.

[3] A. Brosius, H. Karbasian, A. E. Tekkaya, J. Lechler, M. Merklein, M. Geiger, R. Springer, M. Schaper, Fr.-W. Bach, H. So, and H. Hoffmann. Modellierung und Simulation der Warmblechumformung: Aktueller Stand und zukünftiger Forschungsbedarf. In *2. Erlanger Workshop Warmblechumformung*, pages 37–58, 2007.

[4] M. Merklein, J. Lechler, and Geiger M. Characterisation of the flow properties of the quenchable ultra high strength steel 22MnB5. In *CIRP Annals 2006 - Manufacturing Technology*, volume 55/1, pages 229–232, 2006.

[5] M. Eriksson, M. Oldenburg, M. C. Somani, and L. P. Karjalainen. Testing and evaluation of material data for analysis of forming and hardening of boron steel components. *Modelling and Simulation in Materials Science and Engineering*, 10(3):277–294, 2002.

[6] M. Naderi, J.-R. Klepaczko, and W. Bleck. Constitutive modeling of the flow stress during isothermal and non-isothermal forming at high temperatures. *Journal of Materials Processing Technology*, 2007.

[7] L. Burkhardt. *Eine Methodik zur virtuellen Beherrschung thermo-mechanischer Produktionsprozesse bei der Karosserieherstellung*. PhD thesis, ETH Zürich, 2008.

[8] P. F. Bariani, T. Dal Negro, and S. Bruschi. Testing and modelling of material reponse to deformation in bulk metal forming. In *CIRP Annals 2004 - Manufacturing Technology*, volume 53/2, pages 573–595, 2004.

[9] S. Nemat-Nasser. Experimentally-based micromechanical modeling of metal plasticity with homogenization from micro- to macro-scale properties. In O. T. Bruhns and E. Stein, editors, *IUTAM Symposium on Micro- and Macrostructural Aspects of Thermoplasticity*, pages 101–113. Kluwer Academic Publishers, 1999.

[10] P. Åkerström and M. Oldenburg. Studies of the thermo-mechanical material response of a boron steel by inverse modelling. *Journal de Physique IV*, 120:625–633, 2004.

© 2009 Copyright by DYNAmore GmbH

[11] A. Wahlen, U. Feurer, and J. Reissner. Computer controlled measurement and analytical modelling of flow stresses during hot deformation of the copper alloy CuZn42Mn2. *Journal of Materials Processing Technology*, 63:233–237, 1997.

[12] L. Tong, S. Stahel, and P. Hora. Modeling for the FE-simulation of warm metal forming processes. In L. M. Smith, F. Pourboghrat, Yoon J.-W., and T. B. Stoughton, editors, *NUMISHEET 2005 - Proceedings of the 6th International Conference and Workshop on Numerical Simulation of 3D Sheet Metal Froming Processes*, volume 778, pages 625–629. American Institute of Physics, 2005.

[13] J. O. Hallquist. *LS-DYNA Keyword User's Manual - Version 971*. Livermore Software Technology Corporation, May 2007.

[14] N. Stander, R. Willem, T. Goel, T. Eggleston, and K. Craig. *LS-OPT User's Manual*. Livermore Software Technology Corporation, June 2008.

© 2009 Copyright by DYNAmore GmbH